Two-stage Blind Deconvolution

Md. Mafijul Islam Bhuiyan, University of Alberta, Edmonton, Canada
mbhuiyan@ualberta.ca
and
Mauricio D. Sacchi, University of Alberta, Edmonton, Canada

Summary

In seismic data processing, deconvolution plays a very important role because it permits to increase the temporal resolution of seismic sections and to equalize sources. The deconvolution problem when the wavelet is known is an ill-posed problem that can be tackled via regularization methods. However, the seismic source wavelet is unknown and therefore, it must be estimated from the data prior to deconvolution. In this paper, we examine an algorithm to simultaneously estimate the reflectivity and the wavelet. The method assumes that the underlying seismic reflectivity is a sparse series and that a common seismic wavelet exists for a large number of seismograms with different reflectivity sequences. The method reduces to the alternating minimization of a cost function to promote sparsity in the reflectivity and smoothness in the wavelet.

Introduction

In seismic data exploration, deconvolution is used to estimate, from the observed data, the reflectivity series of the subsurface. In general, deconvolution methods assume that the wavelet is known or that it can be estimated from data via the minimum phase assumption (Robinson, 1967; Peacock and Treitel, 1969; Robinson and Treitel, 1980). It can be shown that for a Gaussian white reflectivity series one cannot estimate the phase of the wavelet. In fact, one can only estimate the amplitude spectrum and utilize the minimum phase assumption to estimate the wavelet. However, it can be shown that phase and amplitude of the wavelet can be estimated using higher-order statistical methods when the reflectivity sequence is white and non-Gaussian. Methods in this category are Minimum Entropy Methods (Wiggins, 1978; Donoho, 1991)) and Cumulant Matching techniques (Tugnait, 1997).

We explore an extension of the method proposed by Canadas (2002) for the simultaneous estimation of the wavelet and the reflectivity series that characterize the subsurface. However, there is an important distinction in our method with respect to the method proposed by Canadas (2002), we estimate a wavelet perturbation and not the wavelet in each iteration. We examine the performance of the algorithm versus SNR and the degree of sparsity of the reflectivity. We also provide a marine real data example where we compare the estimated wavelet with the first break wavelet estimator computed by averaging traces of a constant offset section.

The article is organized as follows. First we review the principles of deconvolution method. Next, we introduce the proposed two-stage blind deconvolution algorithm. Eventually, we examine the synthetic and real data examples to manifest the effectiveness of the proposed blind deconvolution technique.

Theory

The seismic trace $d[n]$ can be expressed as the convolution of the reflectivity sequence $r[n]$ and a wavelet $w[n]$ plus a noise contamination term $e[n]$. This system can be represented in matrix-vector

form via the following expression

$$\begin{aligned} \mathbf{d} &= \mathbf{W}\mathbf{r}+\mathbf{e} \quad (1)\\ &= \mathbf{R}\mathbf{w}+\mathbf{e}, \quad (2)\end{aligned}$$

where $\mathbf{d}$ is the N vector of observations, $\mathbf{r}$ is the $M\times 1$ vector representing the reflectivity and $\mathbf{w}$ is the $L\times 1$ vector containing the wavelet coefficients. Similarly, the matrix $\mathbf{W}$ is the $N\times M$ convolution matrix of the wavelet and $\mathbf{R}$ is the $N\times L$ convolution matrix of the reflectivity. Clearly, we have used the commutative property of the discrete convolution where $\mathbf{W}\mathbf{r}=\mathbf{R}\mathbf{w}$. Moreover, we also need to use the familiar expression $M=N+L-1$ that must be honored to properly represent discrete convolution in matrix-vector multiplication form. The above expression easily can be extended in the multichannel problem where we assume a common wavelet for J number of traces. In addition, we assume that the wavelet can be written as the summation of an initial wavelet $\mathbf{W}_0$ and a wavelet perturbation $\Delta\mathbf{W}$. Now, to estimate the reflectivity series ($\mathbf{r}$) and wavelet perturbation ($\Delta\mathbf{w}$) from the multi-channel seismic signal, the following cost function needs to be minimized

$$\psi(\Delta\mathbf{W},\mathbf{r}_1,\mathbf{r}_2,\ldots,\mathbf{r}_J) = \sum_{j=1}^{J}||(\mathbf{W}_0+\Delta\mathbf{W})\,\mathbf{r}_j-\mathbf{d}_j||_2^2+\sum_{j=1}^{J}\lambda||\mathbf{r}_j||_1+\mu||\Delta\mathbf{w}||_2^2. \quad (3)$$

The matrix $\Delta\mathbf{W}$ is the convolution matrix of wavelet perturbation while $\Delta\mathbf{w}$ indicates the perturbation of the wavelet in vector form. The ℓ_2 norm in equation (3) represents the misfit of all traces. This is a non-linear optimization problem and we propose an iterative method where we minimize (ψ) with respect to $\mathbf{r}_j$ and $\Delta\mathbf{w}$. We first minimize with respect to the reflectivity sequence leading to the following system of non-linear equations

$$\frac{\partial\psi}{\partial\mathbf{r}_j}=\mathbf{W}^T\mathbf{W}\mathbf{r}_j-\mathbf{W}^T\mathbf{d}_j+\lambda\mathbf{Q}_j=0,\;\; j=1,\ldots,J, \quad (4)$$

where $\mathbf{Q}_j$ is a diagonal matrix with elements given by the absolute value of the reflectivity samples for trace j. Equation (4) can be solved by applying the Fast Iterative Shrinkage Thresholding Algorithm (FISTA) (Beck and Teboulle, 2009) or Iterative Reweighed Least Squares (IRLS) (Nelder and Wedderburn, 1972). Notice that we need to use the l_1 regularization term to impose sparsity on the reflectivity. It can be shown that the last assumption (sparsity) is vital to operate with this algorithm. We now differentiate the cost function (ψ) with respect to the wavelet perturbation and equate the derivative to zero to obtain condition to estimate the wavelet for fixed reflectivity sequences. It leads to the well-known regularized multichannel least-squares estimator of the wavelet perturbation

$$\Delta\mathbf{w}=(\sum_{j=1}^{J}\mathbf{R}_j^T\mathbf{R}_j+\mu\mathbf{I})^{-1}(\sum_{j=1}^{J}\mathbf{R}_j^T(\mathbf{d}_j-\mathbf{R}_j\mathbf{w}_0)). \quad (5)$$

In the proposed algorithm we start with an initial wavelet and use FISTA to estimate a sparse group of reflectivity sequences (equation 4). With the current estimate of the reflectivity we estimate a wavelet perturbation common to all traces via equation (5). The updated wavelet is filtered with a bandpass filter to guarantee that the wavelet does not have frequency components outside an a priori defined spectral band. The latter is required to stabilize the algorithm and avoid rough estimators of the wavelet. The updated wavelet is then used to re-estimate sparse reflectivity series and so on. The iterative process continues until the wavelet perturbation becomes small enough and the cost function stops changing with iterations. The method will work efficiently with highly uncorrelated spatial reflectivity series. In cases with smooth spatial variations of the reflectivity, one can use the Block Bootstrap (Paparoditis and Politis, 2001) method to generate windows of data with spatially incoherent reflectivity sequences.

Examples

To investigate the performance of the proposed nonlinear optimization algorithm, the correlation of the estimated wavelet with the original one is set as the metric for synthetic seismic data examples. To begin with, a synthetic seismic data is constructed by convolving a sparse reflectivity series with a Ricker wavelet of 60^0 phase rotation. Subsequently, Gaussian and incoherent noise ($SNR = 6$) is added to data. The reflectivity series is portrayed in Figure (1(a)) and the seismic data in Figure (1(b)). The estimated reflectivity calculated by the proposed method is shown in Figure (1(c)). Finally, Figure 2 shows the starting wavelet adopted by our algorithm, the true wavelet and the final estimator of the wavelet.

In order to examine the behaviour of the algorithm under different SNRs and density of reflectors, we have executed 100 realizations of reflectivity sequences and additive noise. The correlation between the true and estimated wavelet is computed for the 100 realizations of synthetic data for each SNR while the density of reflector is kept constant at 40% (meaning 40% samples of the reflectivity are non-zero). The results are shown in Figure (3(a)) which shows the algorithm is quite vulnerable to additive noise. Finally, Figure (3(b)) shows the correlation between the true and estimated wavelet for fixed phase rotation (60^0) and $SNR = 6$ for the case where we varied the density of the reflectivity. The figure manifests that the method works well when the reflector is sparse and starts to break for reflectivity sequences that are non-sparse.

A windowed section from the Mississippi Canyon marine data set was used for testing the algorithm in a real data scenario (Figure (4(a))). The proposed algorithm was applied to calculate the estimated mixed-phase wavelet and reflectivity series. Subsequently, the seismic data was recovered by convolving the estimated wavelet and reflectivity series. Figure (4(b)) depicts the estimated reflectivity series and Figure (4(c)) represents the recovered seismic data. Eventually, Figure 5 shows the comparison among the estimated, average first-break and initial wavelet for real data.

Conclusion

In this article we have formulated a nonlinear optimization algorithm for estimating sparse reflectivity series and a wavelet perturbation. We have initiated the algorithm with a zero phase wavelet and assuming that the reflectivity series is non-gaussian. The proposed algorithm estimates the wavelet perturbation required to update the wavelet and to estimate the sparse reflectivity. Synthetic and real data examples showed that the method was successful to estimate the wavelet and the reflectivity in situations where one can assume high SNR and sparse reflection sequences. The method also requires that the window of analysis contains sufficient spatial variability of the reflectivity sequence.

Acknowledgements

The authors are grateful to Signal Analysis and Imaging Group (SAIG) at the University of Alberta.

References

Beck, A. and M. Teboulle, 2009, A fast iterative shrinkage- thresholding algorithm for linear inverse problem: SIAM J. Imaging Sciences, **Vol.2**, PP. 183–202.

Canadas, G., 2002, A mathematical framework for blind deconvolution inverse problems: Presented at the SEG Int'l Exposition.

Donoho, D., 1991, On minimum entropy deconvolution: Academic press.

Nelder, J. and R. Wedderburn, 1972, Generalized linear models: Journal of Royal Sta..L. Soc., **135**, 370–384.

Paparoditis, E. and D. N. Politis, 2001, Tapered block bootstrap: Biometrika, **88**, pp.1105–1119.

Peacock and Treitel, 1969, Predictive deconvolution: Theory and practice.: Geophysics, **34**, 155Ű169.

Robinson, 1967, Predictive deconvolution of time series with application to seismic exploration: Geophysics, **32**, 418Ű484.

Robinson and Treitel, 1980, Geophysical signal analysis.: Prentice Hall, Inc.

Tugnait, J., 1997, Identification and deconvolution of multichannel linear non-gaussian processes using higher order statistics and inverse filter criteria: Signal Processing, IEEE Transactions on, **45**, 658 – 672.

Wiggins, R. A., 1978, Minimum entropy deconvolution: Geoexploration, **16**, 21–35.

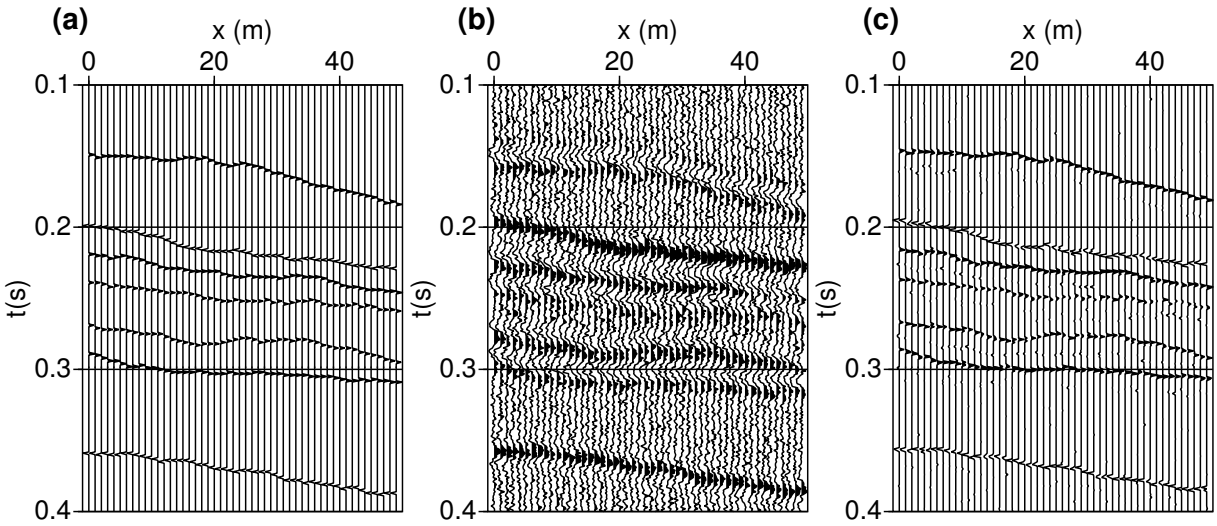

Figure 1 *Synthetic data example. (a) Original reflectivity series utilized to test the proposed blind deconvolution algorithm. (b) Seismic data modelled by convolution of the reflectivity with a Ricker wavelet with phase rotation* 60^0*. The data were also contaminated with noise (SNR = 6.0). (c) Sparse reflectivity series obtained by the proposed blind deconvolution method.*

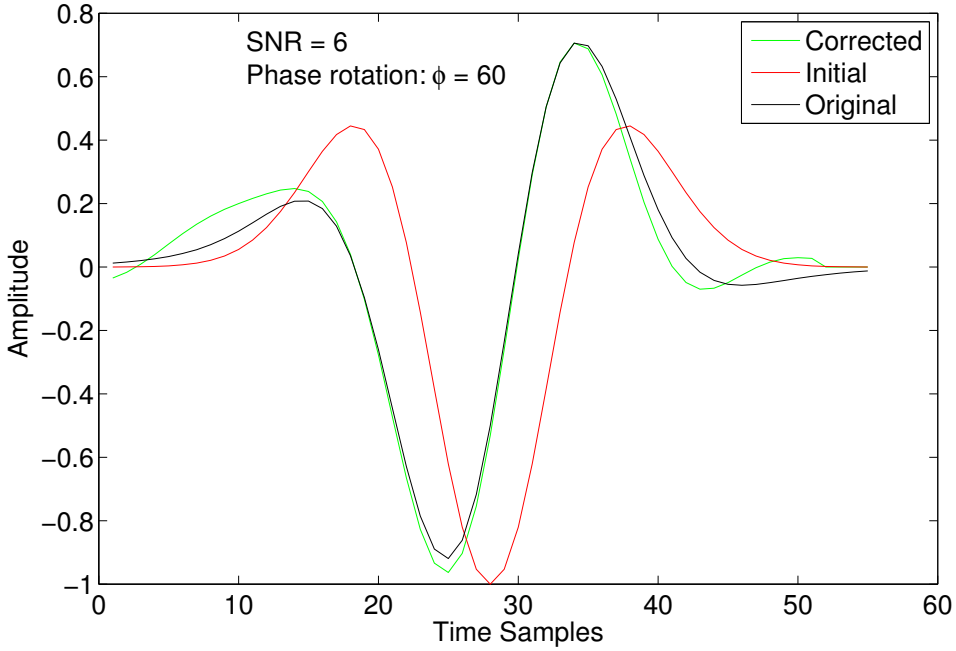

Figure 2 *Initial, original, and estimated wavelet for synthetic data with phase rotation* 60^0 *and SNR=6.*

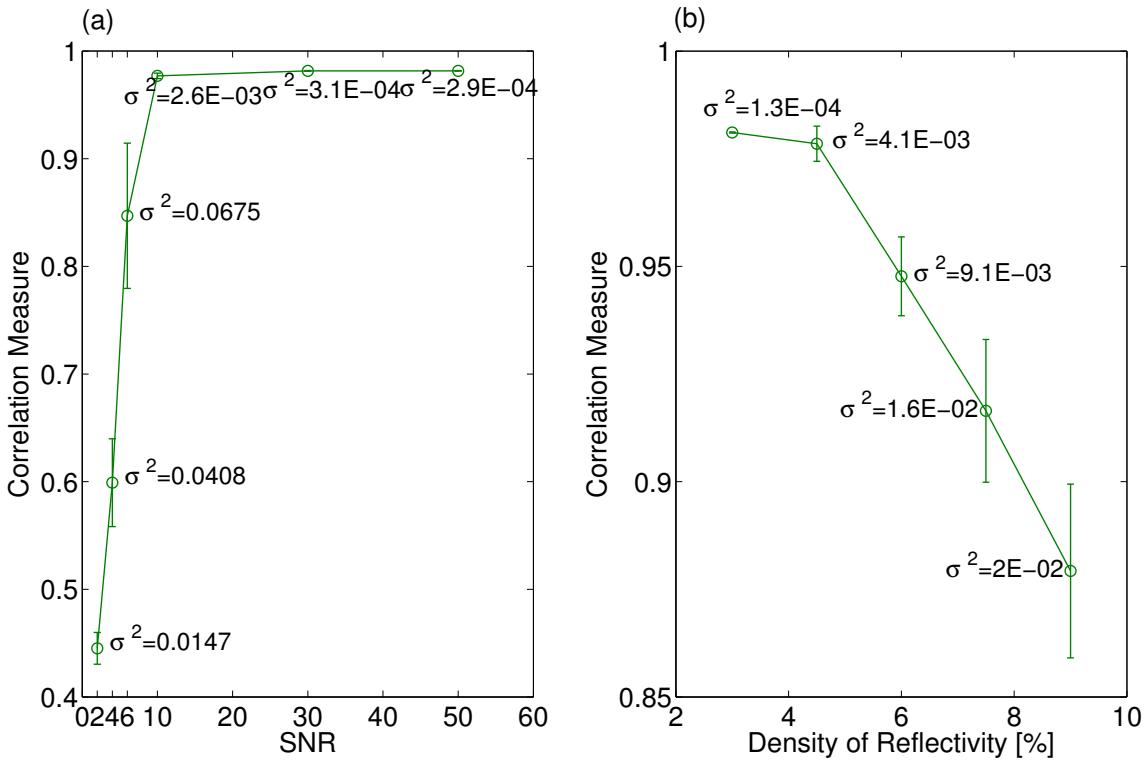

Figure 3 *The normalized correlation between the estimated and true wavelet for different (a) SNRs and (b) density of reflectors (the density measures the percentage of non-zero coefficients of the reflectivity series).*

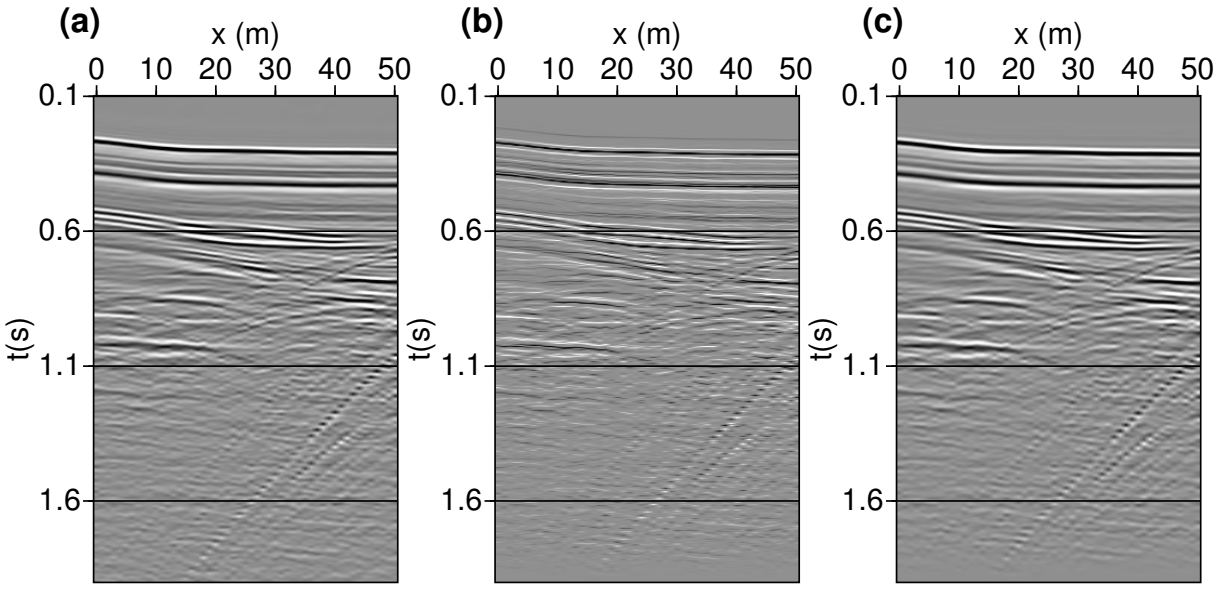

Figure 4 *Real data example. (a) A window of the Mississippi Canyon marine seismic data. (b) Reflectivity series estimated via the proposed algorithm. (c) Seismic data after convolution of the estimated reflectivity with the estimated wavelet.*

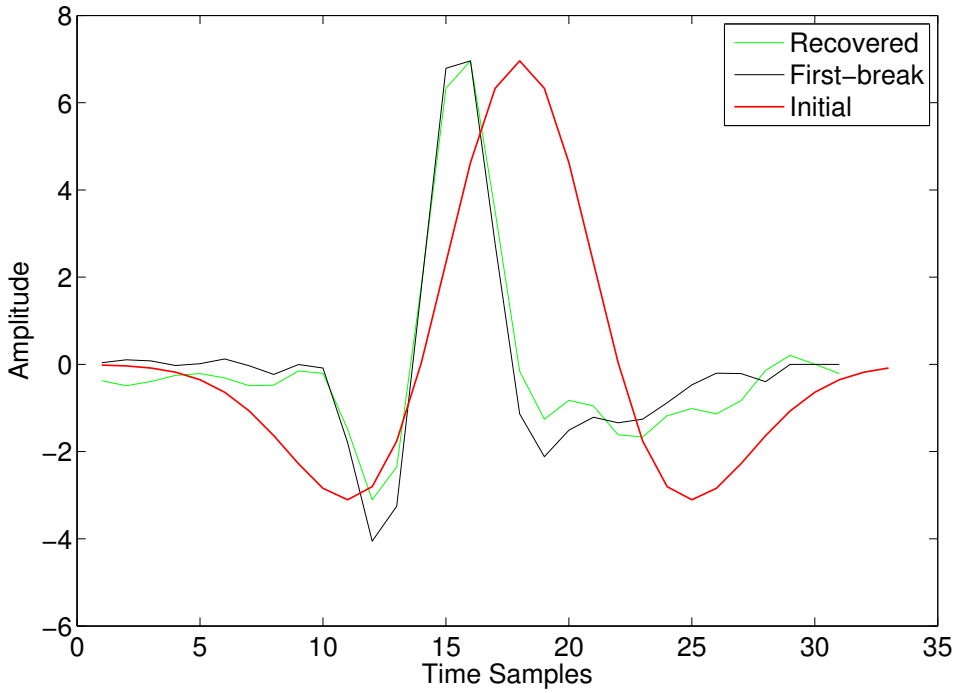

Figure 5 *Initial, recovered, and first-break wavelet for real data.*